A mouse model of heterogeneous, c-MYC-initiated prostate cancer with loss of *Pten* and *p53*

Jongchan Kim, Ph.D.[1], **Meejeon Roh, Ph.D.**[1], **Irina Doubinskaia, M.S.**[1], **Gabriela N. Algarroba**[1,2], **Isam-Eldin A. Eltoum, M.D.**[3], and **Sarki A. Abdulkadir, M.D., Ph.D.**[*,1]

[1]Department of Pathology, Vanderbilt University Medical Center, Nashville, Tennessee, United States of America

[2]College of Agricultural and Life Sciences, University of Florida at Gainesville, Gainesville, Florida, United States of America

[3]Department of Pathology, University of Alabama at Birmingham, Birmingham, Alabama, United States of America

Abstract

Human tumors are heterogeneous and evolve through a dynamic process of genetic mutation and selection. During this process, the effects of a specific mutation on the incipient cancer cell may dictate the nature of subsequent mutations that can be tolerated or selected for, affecting the rate at which subsequent mutations occur. Here we have used a new mouse model of prostate cancer that recapitulates several salient features of the human disease to examine the relative rates in which the remaining wild type alleles of *Pten* and *p53* tumor suppressor genes are lost. In this model, focal overexpression of c-MYC in a few prostate luminal epithelial cells provokes a mild proliferative response. In the context of compound *Pten/p53* heterozygosity, c-MYC-initiated cells progress to prostatic intraepithelial neoplasia (mPIN) and adenocarcinoma lesions with marked heterogeneity within the same prostate glands. Using Laser Capture Microdissection and gene copy number analyses, we found that the frequency of *Pten* loss was significantly higher than that of *p53* loss in mPIN but not invasive carcinoma lesions. c-MYC overexpression, unlike *Pten* loss, did not activate the p53 pathway in transgenic mouse prostate cells, explaining the lack of selective pressure to lose *p53* in the c-MYC-overexpressing cells. This model of heterogeneous prostate cancer based on alterations in genes relevant to the human disease may be useful for understanding pathogenesis of the disease and testing new therapeutic agents.

Keywords

c-MYC; Pten; p53; prostate cancer; rate of mutations

*To whom correspondence should be addressed. Medical Center North, Rm B3321, Vanderbilt University School of Medicine, Nashville, TN 37232, sarki.abdulkadir@vanderbilt.edu, Tel: (615) 322-9668, Fax: (615) 343-7023.

Disclosure of Potential Conflicts of Interest

The authors declare no conflict of interest.

Introduction

Human somatic tumorigenesis is believed to initiate with a single genetic mutation in a cancer gene, with progressive accumulation of additional genetic alterations that confer a selective growth advantage on the mutant cell (Fearon & Vogelstein, 1990). A notable feature of this multistep model of carcinogenesis is the occurrence of a preferred (but not absolute) order in which these genetic mutations accumulate during cancer progression (Fearon & Vogelstein, 1990; Yeang et al., 2008). In human colorectal carcinomas where defined histopathological stages are easily recognizable and accessible, this notion could be examined (Fearon & Vogelstein, 1990). However, other tumors such as prostate cancer, are notoriously heterogeneous and have precursor lesions that are not as well defined (Andreoiu & Cheng,; Cheng et al., 1998; Greene et al., 1991; Villers et al., 1992). Some have suggested that prostate cancer heterogeneity may be due to an underlying "field effect" which sensitizes wide swathes of tissue to transformation without the presence of an obvious histological abnormality, a phenomenon known as field cancerization (Slaughter et al., 1953). This complexity of the human disease makes the use of accurate animal models an attractive approach to define tumor initiation and multistep progression in prostate cancer.

To begin to address these issues, we used the *Z-MYC* mouse (Roh et al., 2006) which contains a latent, Cre-activatable *c-MYC* allele which when combined with a prostate-specific Cre allele (*PbCre4*), yields a novel mouse model of c-MYC-initiated prostate cancer that recapitulates various salient features of the human disease (Kim et al., 2009). In the *PBCre4;Z-MYC* model, we have shown that c-MYC is induced focally in the prostatic luminal epithelial cells. Notably, in a significant fraction of these mice, c-MYC expression leads to the expansion of "fields" of c-MYC-positive cells without eliciting any obvious pathology (Kim et al., 2009). However, c-MYC expression sensitizes the prostate cells to the transforming effects of additional mutations. To examine tumor progression in this model, we have generated *Pten/p53* compound mutant mice and examined loss of gene copy number in microdissected c-MYC-expressing prostate lesions. The genes that form the basis for this mouse model are relevant to human prostate cancer. c-MYC overexpression is an early event in prostate cancer, with recent studies indicating overexpression in up to ~76% of prostatic intraepithelial neoplasia (PIN) lesions (Gurel et al., 2008), while alterations in *PTEN* and *P53* have been observed in human prostate cancer with varying frequencies (Bookstein et al., 1993; Brooks et al., 1996; Carver et al., 2009; Chi et al., 1994; Dinjens et al., 1994; Dong et al., 2001; Effert et al., 1993; Feilotter et al., 1998; Fenic et al., 2004; Fernandez-Marcos et al., 2009; Grizzle et al., 1994; Han et al., 2009; Konishi et al., 1995; McCall et al., 2008; McMenamin et al., 1999; Mellon et al., 1992; Mirchandani et al., 1995; Navone et al., 1993; Nesslinger et al., 2003; Qian et al., 2002; Schmitz et al., 2007; Sircar et al., 2009; Suzuki et al., 1998; Voeller et al., 1994; Wang et al., 1998; Yoshimoto et al., 2007). However, there has been limited analysis of the rates of mutation in *PTEN* and *P53* in the same tumor, and their relation to progression. Our analysis of c-MYC-initiated mouse prostate tumors allowed examination of alterations in *Pten* versus *p53* during tumor progression, which appears to be dictated by the molecular interaction between the c-MYC, Pten and p53 pathways.

Materials and Methods

Animals

Z-MYC, *PbCre4*, *Pten^{f/f}* and *p53^{f/f}* mice on B6/129 background have been described previously (Groszer et al., 2001; Jonkers et al., 2001; Kim et al., 2009; Roh et al., 2006; Wu et al., 2001). *p53^{f/f}* and *Pten^{f/f}* mice were obtained from MMHCC, Frederick. *PbCre4;p53^{f/+}*, *PbCre4;p53^{f/f}*, *PbCre4;Z-MYC;p53^{f/+}* and *PbCre4;Z-MYC;p53^{f/f}* mice were generated using a similar strategy to that described for generating *PbCre4/Z-MYC/Pten^{f/f}* compound mutant mice (Kim et al., 2009). To generate *PbCre4;Pten^{f/+};p53^{f/+}*, *PbCre4;Pten^{f/f};p53^{f/+}*, *PbCre4;Pten^{f/+};p53^{f/f}*, *PbCre4;Z-MYC;Pten^{f/+};p53^{f/+}*, *PbCre4;Z-MYC;Pten^{f/f};p53^{f/+}*, *PbCre4;Z-MYC;Pten^{f/+};p53^{f/f}* mice, we first generated *PbCre4;Pten^{f/f};p53^{f/f}* males and *Z-MYC;Pten^{f/+};p53^{f/+}* females and these were further crossed. Animal care and experiments were carried out according to the protocols approved by the Institutional Animal Care and Use Committees at Vanderbilt University.

Histology and immunohistochemical analyses

Mouse prostate tissues were prepared as described (Abdulkadir et al., 2001b) and histopathology was evaluated by SAA and IAE based on published criteria (Mentor-Marcel et al., 2001). Immunohistochemical analyses were performed as described (Abdulkadir et al., 2001a)(Abdulkadir et al., 2001b) and the following antibodies were used (when indicated as TSA, Tyramide Signal Amplification (Perkin Elmer) was applied): anti-c-MYC (rabbit, 1:15,000 with TSA, Santa Cruz Biotechnology), anti-α-smooth muscle actin (SMA) (mouse, 1:2000, Sigma), anti-Pten (rabbit, 1:200 with TSA, Cell Signaling), anti-Synaptophysin (mouse, 1:1000, BD Biosciences), anti-activated Caspase 3 (rabbit, 1:500, Cell Signaling), anti-phospho-Histone H3 (rabbit, 1:500, Upstate), anti-p53 (rabbit, 1:5000 with TSA, Santa Cruz Biotechnology) and anti-androgen receptor (AR) (rabbit, 1:500, Santa Cruz Biotechnology). Double stains with two antibodies of same species are described previously (Kim et al., 2009). 3–4 tissue samples were used for the quantitation of proliferation and apoptosis using anti-phospho-Histone H3 and anti-activated Caspase 3 antibodies. Nuclei were stained with DAPI (Vector Laboratories).

Laser capture microdissection (LCM) and DNA isolation

LCM was performed on PixCell II Laser Capture Microdissection System (MDS) using CapSure Macro LCM Caps (MDS) and DNA extraction was followed according to manufacturer's instruction (PicoPure DNA extraction kit, MDS). Immunostaining for c-MYC and Pten on adjacent sections were used to guide LCM.

Quantitative Polymerase Chain Reaction (qPCR) and Gene copy number analysis

QPCR with extracted DNA from LCM procedure was performed on 7300 Real Time PCR System (Applied Biosystems) using Platinum qPCR Supermix-UDG (Invitrogen). For the reaction of 25μl, 12.5μl of 2× Supermix, 1.4μl of water, 0.5μl of ROX reference dye, 1μl each of two 6μM primer pairs (*Pten/Apo B* or *p53/Apo B*), 0.8μl each of two 6μM probes (*Pten/Apo B* or *p53/Apo B*) and 5μl of DNA were added. *Apo B* gene was always coamplified with either *Pten* or *p53* as an internal control. Mouse tail DNA was included in

each reaction for normalization. Conditional *Pten* heterozygous and *p53* heterozygous prostate tissues were used as standard samples to determine the range of gene copy number (1 or 0). Triplicate data were analyzed by ddCt method. Based on the range of normalized quantity of standard samples (0.451–0.679 for one copy of *Pten* and 0.276–0.462 for one copy of *p53*, see Table S1) as well as significance *t*-test ($P < 0.05$) between normalized sample quantities and standard sample quantities, gene copy numbers of *Pten* and *p53* were determined. Primers and probes used were: *Pten* forward (5'-ACA ATC ATg TTg CAg CAA TTC AC-3'), *Pten* reverse (5'-CCg ATg CAA TAA ATA TgC ACA AA-3') and *Pten* probe (5'-/FAM/CCg gAT g AgC Tgg AAA ggg ACg gAC Tgg TgT AA CAT CCg g/ BHQ/-3'); *Apo B* forward (5'-ATC TCA gCA CgT ggg CTC-3'), *Apo B* reverse (5'-TCA CCA gTC ATT TCT gCC TTT g-3') and *Apo B* probe (5'-/JOE/CgC gAT g CCA ATg gTC ggg CAC TgC TCA A CAT CgC g/BHQ/-3'); *p53* forward (5'-CTg TgC AgT TgT ggg TCA gC-3'), *p53* reverse (5'-ACC TCC gTC ATg TgC TgT gA-3') and *p53* probe (5'-/FAM/CCg gAT g ggA gCC gTg TCC gCg CCA T CAT CCg g/BHQ/-3') (all sequences are available at http://emice-stage.nci.nih.gov/).

Statistical analyses

Each group was compared using *t*-test or *Chi*-square test (Preacher, 2001). Values are considered statistically significant at $P < 0.05$. Quantitative variables are expressed as means ± standard deviation while categorical variables are expressed as numbers (%).

Results

c-MYC expression sensitizes prostate cells to the effects of loss of one or both copies of the *p53* tumor suppressor gene (TSG)

Our primary goal was to generate a focal, stepwise model of prostate cancer that closely resembles the human disease and in which we can investigate the relative frequencies of TSG (*Pten* and *p53*) loss at various stages of progression. We have previously shown that focal c-MYC expression in *Pten* heterozygous mice leads to efficient generation of PIN lesions associated with downregulation of Pten protein expression (Kim et al., 2009). Progression of these c-MYC+;Pten-negative lesions is restrained by an apoptotic response concurrent with activation of the p53 pathway (Kim et al., 2009). To further explore the role of p53 in this model, we first assessed the effects of concurrent loss of *p53* and overexpression of c-MYC. We generated cohorts of conditional, compound mutant mice as follows: *PbCre4;Z-MYC;p53$^{f/+}$* (*c-MYC+;p53-het*), *PbCre4;Z-MYC;p53$^{f/f}$* (*c-MYC+;p53-ko*), *PbCre4;p53$^{f/+}$* (*p53-het*) and *PbCre4;p53$^{f/f}$* (*p53-ko*), where "het" refers to heterozygous and "ko" refers to knockout. In agreement with a previous report (Chen et al., 2005), *p53* deficiency in the mouse prostate by itself did not cause any noticeable abnormalities (Figures 1, 2A and 3). However, concurrent c-MYC expression and heterozygous or homozygous *p53* deletion led to the age-dependent development of low grade PIN (LGPIN) and high grade PIN (HGPIN) (Figures 1, 2A and 3). Some HGPIN lesions in *c-MYC+;p53-ko* mice showed evidence of microinvasion but still retained Pten protein expression (Figure 3B). There was an additive increase in proliferation in cells with concurrent reduction of *p53* dosage and c-MYC expression without a significant change in apoptosis (Figure 3C). This contrasts with *c-MYC+;Pten-ko* prostates which show elevated

rates of apoptosis (Kim et al., 2009). Thus c-MYC expression cooperates modestly with *p53* loss in the prostate but the lesions do not rapidly progress to invasive cancer. Notably, we have shown that the level of c-MYC expression in our *c-MYC+* prostate model is not sufficient to activate the p53 pathway (Kim et al., 2009) (see also Figure S1), possibly explaining the lack of selective pressure to lose *p53* upon c-MYC expression.

Pten and *p53* restrain the progression of c-MYC-initiated prostate cancer

The results from analysis of *c-MYC+;p53*-mutant mice shown above and our previously reported analysis of *c-MYC+;Pten*-mutant mice (Kim et al., 2009) suggest that retention of wild type *Pten* or *p53* restrains the progression of c-MYC-initiated prostate cancer cells with mutation in either the *p53* or *Pten* TSGs. We sought formal proof of this by examining tumor progression in conditional *c-MYC+;Pten/p53* compound mutant mice where only one of either the *Pten* or *p53* alleles is wild type. Indeed, while control *Pten-het;p53-ko* mice without c-MYC overexpression only developed HGPIN with a 33% incidence in mice monitored up to 50 weeks of age (Figures 1, 2B, and 4), *c-MYC+;Pten-het;p53-ko* mice developed aggressive prostate adenocarcinoma as early as 10 weeks of age (Figures 1, 2B and 4). These tumors were associated with downregulation of the wild type Pten expression (Figure 4C) and were metastatic to the lymph nodes as verified by staining for androgen receptor (AR) and cytokeratin 8 (Figure 4B, panels `c–e'). Similarly, *c-MYC+;Pten-ko;p53-het* mice developed aggressive prostate adenocarcinoma while the control *Pten-ko;p53-het* mice developed HGPIN and well-differentiated prostate cancer (Figures 1, 2 and 4), consistent with the reported phenotype of *Pten-ko* mice (Wang et al., 2003). In all cases in these *c-MYC+;Pten-het;p53-ko* and *c-MYC+;Pten-ko;p53-het* compound mutant mice, development of aggressive tumors was associated with loss of the corresponding wild type *Pten* or *p53* allele as determined by gene copy number assessment using c-MYC and Pten immunofluorescence-guided Laser Capture Microdissection (Table 1; see also Figure 7E panels b and c). These results indicate potent synergy between c-MYC expression and loss of *Pten/p53* that appears to be largely mediated by accelerating loss of the wild type *Pten* or *p53* allele. In this regard, it is interesting to note that even in the prostate lesions of *c-MYC +;Pten-ko* (i.e. *PbCre4;Z-MYC;Pten^{f/f}*) mutant mice, we found evidence for loss of 1 or both copies of the wild type *p53* alleles (Figure 7E, panels "b" and "c" and Table S2).

Higher rate of loss of *Pten* compared to *p53* in conditional *c-MYC+;Pten-het;p53-het* mice during prostate tumorigenesis

The heterogeneous focal nature of c-MYC expression in our model provides us with an opportunity to examine, within the same prostate glands, the evolution of PIN lesions to carcinoma and the choice made by incipient neoplastic cells between loss of *Pten* and loss of *p53* during tumor evolution. To facilitate this analysis, we generated and monitored tumor progression in *c-MYC+;Pten-het;p53-het* and control *Pten-het;p53-het* mice. In the absence of c-MYC expression heterozygous deletion of *Pten* and *p53* resulted only in PIN with a low penetrance (Figures 1, 2C and 5). However, in *c-MYC+;Pten-het;p53-het* mice with concurrent focal c-MYC expression, we observed focal heterogeneous lesions including PIN, well-differentiated, moderately-differentiated and poorly-differentiated prostate adenocarcinoma (Figures 1, 2C and 5). The lesions appear to start focally, the neoplastic cells are luminal, AR-positive, without neuroendocrine differentiation and the invasive

process is distinctly clear (Figures 5 and 6). Remarkably the PIN and cancer lesions that develop in these animals showed heterogeneous morphology (Figure 5C) suggesting that the lesions contain distinct combinations of genetic abnormalities. Thus this model captures one of the key features of human prostate cancer, i.e. histopathological heterogeneity.

To determine the rates at which *Pten* and *p53* are lost during the progression of these c-MYC-initiated lesions, we used immunofluorescence-guided LCM followed by gene copy number analysis. We stained serial sections from *c-MYC+;Pten-het;p53-het* mice for c-MYC, Pten and H&E for LCM (Figure 7). All lesions analyzed demonstrated c-MYC expression. We determined *Pten* and *p53* gene copy numbers by qPCR with DNA isolated following LCM from a total of 60 PIN and cancer foci (Tables 1 and S1). Overall, *Pten* copy loss was observed in 60% of the PIN and cancer lesions while *p53* was lost in 40% of the lesions (Table 1, Figure 7E). Notably, the rate of *Pten* copy number loss is significantly higher than that of *p53* loss in PIN lesions (50% vs. 29.2%), while cancer lesions showed equivalent rates of *Pten* and *p53* loss (Table 1, Figure 7D). Furthermore, samples with *p53* loss were subsumed in those with *Pten* loss with two exceptions (samples S35 and S76 in Table 1). These results indicate a higher rate of *Pten* loss compared to *p53* loss during mouse prostate tumor progression.

We were also able to correlate loss of Pten protein expression in the same prostatic glands to loss of *Pten* copy number (Figure 7A, B). There were more lesions with loss of Pten expression than with *Pten* loss of copy number (Figure 7B). Thus, only 70.6% (36/51) of the lesions with loss of Pten expression showed evidence for loss of *Pten* copy number as well (Figure 7B). For example, in Figure 7A, while both lesions S3 and S4 displayed loss of Pten expression, only S4 also showed loss of *Pten* gene copy. While it is difficult to completely exclude the possibility of stromal contamination of LCM material, these results may also indicate the fact that loss of Pten protein precedes genetic loss of *Pten* DNA, through epigenetic mechanisms including promoter methylation (Cheung et al., 2004; Wang et al., 2007) or post-transcriptional/-translational control of Pten mRNA/protein (Sansal & Sellers, 2004).

Discussion

Our model of prostate cancer based on conditional focal c-MYC expression in the mouse prostate epithelium recapitulates several salient aspects of the human disease. First, all the three genes we focused on, i.e. *c-MYC*, *Pten* and p*53* are frequently involved in human prostate cancer, with c-MYC overexpression being the most early and most frequent alteration of the three genes (Gurel et al., 2008; Taylor et al., 2010). Second, c-MYC+ cells in this model expand over time to form a field of histologically normal, c-MYC-overexpressing cells that are sensitized to the effects of further tumorigenic mutations, specifically loss of one or both alleles of *Pten* or *p53*. The fact that histologically normal-appearing tissue may harbor cancer-promoting alterations raises questions about the appropriateness of using so-called "normal adjacent prostate" as a control in molecular studies aimed at deciphering differences between cancer and normal tissues. Third, in the *c-MYC+;Pten-het;p53-het* model, PIN and cancer lesions arise focally and are histologically heterogeneous, even within the same glands. This most likely reflects the genetic

heterogeneity of lesions, as *c-MYC*+;*Pten*-deficient lesions are histologically quite distinct from *c-MYC*+;*p53*-deficient lesions. Fourth the tumors that arise in this model are adenocarcinomas like the majority of human prostate cancers, retaining androgen receptor expression with no evidence of significant neuroendocrine differentiation.

The *c-MYC*+;*Pten-het;p53-het* model provided a unique opportunity to examine the rate at which distinct TSGs are lost during prostate tumor progression. The heterozygosity in *Pten* and *p53* facilitates analysis of TSG pathway inactivation, making it more likely that the tumors will select loss of the wild type TSG allele as a means of inactivating the pathway, rather than mutations in other components of the pathway that may have the same functional outcome. Indeed, our finding that advanced tumors in this model uniformly show loss of *Pten* and *p53* genes validates this approach. In human tumors, evidence for a preferred order in which mutations in cancer genes develop during clonal progression have been deduced by examining the mutation frequencies for various genes at different stages of tumor progression and the rate in which mutations in specific genes co-occur (Fearon & Vogelstein, 1990); (Yeang et al., 2008).

Using, LCM we examined a large number of PIN and cancer lesions for status of the wild type *Pten* and *p53* alleles in *c-MYC*+;*Pten-het;p53-het* mice and found clear evidence for a preference for the loss of *Pten* prior to *p53*. Examination of human samples supported with this conclusion. These results indicate that while the mutations involved in tumor initiation may arise stochastically, the nature of the subsequent genetic alterations selected for during clonal evolution may be constrained by the nature of the preceding mutation. Thus, c-MYC overexpressing cells tend to lose *Pten* over *p53* because loss of *Pten* provides greater selective advantage to the tumor cell than *p53* loss (Figure 8). Additionally, c-MYC overexpression in our model does not activate p53, meaning there is no pressure on the c-MYC+ cells to inactivate the p53 pathway. Once *Pten* is lost however, the p53 pathway is strongly activated (Chen et al., 2005; Kim et al., 2009). In the context of c-MYC overexpression in our model, we have shown that the p53 response is shifted from senescence to apoptosis because c-MYC represses the p53 target gene *p21^{Cip1}* (Kim et al., 2009). Thus Pten loss, even though it provides several advantages to the tumor cell also activates a tumor-restraining barrier in the form of p53 activation. This provides selective pressure for inactivation of *p53*. Indeed we found that advanced prostate cancers in *c-MYC*+;*Pten-het;p53-het* mice show almost uniform evidence of loss of the wild type *p53* allele.

It is important to point out that our Z-MYC model differs from other prostate-Myc transgenic models that have been analyzed. For example, De Marzo and colleagues (Iwata et al., 2010) recently analyzed Lo-Myc and Hi-Myc transgenic mice developed by the Sawyers group (Ellwood-Yen et al., 2003) and deduced that MYC overexpression leads to an immediate change in cellular morphology consistent with transformation. We do not see a similar effect in our prostate Z-MYC model, possibly due to differences in expression level or genetic strain differences.

Our study has not directly addressed the cell of origin of the tumors in this model. Our previous analysis of the *PBCre4*;*Z-MYC* model has shown that c-MYC is induced focally in the prostatic luminal epithelial cell compartment (Kim et al., 2009). The specific identity of

Author Manuscript

the cell of origin of the tumors that develop in this model awaits further study. Nonetheless, it may be possible, once the rules governing the timing and rate at which mutations occur during tumor progression are understood, to exploit them in individualized chemopreventive or therapeutic strategies to the detriment of the tumor cell. For example, *c-MYC+;Pten*-deficient tumor cells are under pressure to avoid a strong p53-dependent apoptotic response, and this knowledge could be exploited. Such efforts will be crucially dependent on the use of accurate *in vivo* models of human cancer like the *c-MYC+;Pten-het;p53-het* mouse model described here.

Supplementary Material

Refer to Web version on PubMed Central for supplementary material.

Acknowledgements

Abbreviations

PIN	prostatic intraepithelial neoplasia
LCM	laser-captured microdissection
qPCR	quantitative polymerase chain reaction
BHQ	Black Hole Quencher

## References

Abdulkadir SA, Carbone JM, Naughton CK, Humphrey PA, Catalona WJ, Milbrandt J. Hum Pathol. 2001a; 32:935–9. [PubMed: 11567222]

Abdulkadir SA, Qu Z, Garabedian E, Song SK, Peters TJ, Svaren J, Carbone JM, Naughton CK, Catalona WJ, Ackerman JJ, Gordon JI, Humphrey PA, Milbrandt J. Nat Med. 2001b; 7:101–7. [PubMed: 11135623]

Andreoiu M, Cheng L. Hum Pathol. 41:781–93. [PubMed: 20466122]

Bookstein R, MacGrogan D, Hilsenbeck SG, Sharkey F, Allred DC. Cancer Res. 1993; 53:3369–73. [PubMed: 8324747]

Brooks JD, Bova GS, Ewing CM, Piantadosi S, Carter BS, Robinson JC, Epstein JI, Isaacs WB. Cancer Res. 1996; 56:3814–22. [PubMed: 8706029]

Carver BS, Tran J, Gopalan A, Chen Z, Shaikh S, Carracedo A, Alimonti A, Nardella C, Varmeh S, Scardino PT, Cordon-Cardo C, Gerald W, Pandolfi PP. Nat Genet. 2009; 41:619–24. [PubMed: 19396168]

Chen Z, Trotman LC, Shaffer D, Lin HK, Dotan ZA, Niki M, Koutcher JA, Scher HI, Ludwig T, Gerald W, Cordon-Cardo C, Pandolfi PP. Nature. 2005; 436:725–30. [PubMed: 16079851]

Cheng L, Song SY, Pretlow TG, Abdul-Karim FW, Kung HJ, Dawson DV, Park WS, Moon YW, Tsai ML, Linehan WM, Emmert-Buck MR, Liotta LA, Zhuang Z. J Natl Cancer Inst. 1998; 90:233–7. [PubMed: 9462681]

Cheung TH, Lo KW, Yim SF, Chan LK, Heung MS, Chan CS, Cheung AY, Chung TK, Wong YF. Gynecol Oncol. 2004; 93:621–7. [PubMed: 15196854]

Chi SG, deVere White RW, Meyers FJ, Siders DB, Lee F, Gumerlock PH. J Natl Cancer Inst. 1994; 86:926–33. [PubMed: 7515114]

Dinjens WN, van der Weiden MM, Schroeder FH, Bosman FT, Trapman J. Int J Cancer. 1994; 56:630–3. [PubMed: 8314337]

Dong JT, Li CL, Sipe TW, Frierson HF Jr. Clin Cancer Res. 2001; 7:304–8. [PubMed: 11234884]

Effert PJ, McCoy RH, Walther PJ, Liu ET. J Urol. 1993; 150:257–61. [PubMed: 8510267]

Ellwood-Yen K, Graeber TG, Wongvipat J, Iruela-Arispe ML, Zhang J, Matusik R, Thomas GV, Sawyers CL. Cancer Cell. 2003; 4:223–38. [PubMed: 14522256]

Fearon ER, Vogelstein B. Cell. 1990; 61:759–67. [PubMed: 2188735]

Feilotter HE, Nagai MA, Boag AH, Eng C, Mulligan LM. Oncogene. 1998; 16:1743–8. [PubMed: 9582022]

Fenic I, Franke F, Failing K, Steger K, Woenckhaus J. J Pathol. 2004; 203:559–66. [PubMed: 15095479]

Fernandez-Marcos PJ, Abu-Baker S, Joshi J, Galvez A, Castilla EA, Canamero M, Collado M, Saez C, Moreno-Bueno G, Palacios J, Leitges M, Serrano M, Moscat J, Diaz-Meco MT. Proc Natl Acad Sci U S A. 2009; 106:12962–7. [PubMed: 19470463]

Greene DR, Wheeler TM, Egawa S, Weaver RP, Scardino PT. Br J Urol. 1991; 68:499–509. [PubMed: 1747726]

Grizzle WE, Myers RB, Arnold MM, Srivastava S. J Cell Biochem Suppl. 1994; 19:259–66. [PubMed: 7823598]

Groszer M, Erickson R, Scripture-Adams DD, Lesche R, Trumpp A, Zack JA, Kornblum HI, Liu X, Wu H. Science. 2001; 294:2186–9. [PubMed: 11691952]

Gurel B, Iwata T, Koh CM, Jenkins RB, Lan F, Van Dang C, Hicks JL, Morgan J, Cornish TC, Sutcliffe S, Isaacs WB, Luo J, De Marzo AM. Mod Pathol. 2008; 21:1156–67. [PubMed: 18567993]

Han B, Mehra R, Lonigro RJ, Wang L, Suleman K, Menon A, Palanisamy N, Tomlins SA, Chinnaiyan AM, Shah RB. Mod Pathol. 2009; 22:1083–93. [PubMed: 19407851]

Iwata T, Schultz D, Hicks J, Hubbard GK, Mutton LN, Lotan TL, Bethel C, Lotz MT, Yegnasubramanian S, Nelson WG, Dang CV, Xu M, Anele U, Koh CM, Bieberich CJ, De Marzo AM. PLoS One. 2010; 5:e9427. [PubMed: 20195545]

Jonkers J, Meuwissen R, van der Gulden H, Peterse H, van der Valk M, Berns A. Nat Genet. 2001; 29:418–25. [PubMed: 11694875]

Kim J, Eltoum IE, Roh M, Wang J, Abdulkadir SA. PLoS Genet. 2009; 5:e1000542. [PubMed: 19578399]

Konishi N, Hiasa Y, Hayashi I, Matsuda H, Tsuzuki T, Ming T, Kitahori Y, Shiraishi T, Yatani R, Shimazaki J. Jpn J Cancer Res. 1995; 86:57–63. [PubMed: 7737911]

McCall P, Witton CJ, Grimsley S, Nielsen KV, Edwards J. Br J Cancer. 2008; 99:1296–301. [PubMed: 18854827]

McMenamin ME, Soung P, Perera S, Kaplan I, Loda M, Sellers WR. Cancer Res. 1999; 59:4291–6. [PubMed: 10485474]

Mellon K, Thompson S, Charlton RG, Marsh C, Robinson M, Lane DP, Harris AL, Horne CH, Neal DE. J Urol. 1992; 147:496–9. [PubMed: 1370701]

Mentor-Marcel R, Lamartiniere CA, Eltoum IE, Greenberg NM, Elgavish A. Cancer Res. 2001; 61:6777–82. [PubMed: 11559550]

Mirchandani D, Zheng J, Miller GJ, Ghosh AK, Shibata DK, Cote RJ, Roy-Burman P. Am J Pathol. 1995; 147:92–101. [PubMed: 7604888]

Navone NM, Troncoso P, Pisters LL, Goodrow TL, Palmer JL, Nichols WW, von Eschenbach AC, Conti CJ. J Natl Cancer Inst. 1993; 85:1657–69. [PubMed: 7692074]

Nesslinger NJ, Shi XB, deVere White RW. Cancer Res. 2003; 63:2228–33. [PubMed: 12727844]

Preacher, K. 2001.

Qian J, Hirasawa K, Bostwick DG, Bergstralh EJ, Slezak JM, Anderl KL, Borell TJ, Lieber MM, Jenkins RB. Mod Pathol. 2002; 15:35–44. [PubMed: 11796839]

Roh M, Kim J, Song C, Wills M, Abdulkadir SA. Genesis. 2006; 44:447–53. [PubMed: 17013838]

Sansal I, Sellers WR. J Clin Oncol. 2004; 22:2954–63. [PubMed: 15254063]

Schmitz M, Grignard G, Margue C, Dippel W, Capesius C, Mossong J, Nathan M, Giacchi S, Scheiden R, Kieffer N. Int J Cancer. 2007; 120:1284–92. [PubMed: 17163422]

Sircar K, Yoshimoto M, Monzon FA, Koumakpayi IH, Katz RL, Khanna A, Alvarez K, Chen G, Darnel AD, Aprikian AG, Saad F, Bismar TA, Squire JA. J Pathol. 2009; 218:505–13. [PubMed: 19402094]

Slaughter DP, Southwick HW, Smejkal W. Cancer. 1953; 6:963–8. [PubMed: 13094644]

Suzuki H, Freije D, Nusskern DR, Okami K, Cairns P, Sidransky D, Isaacs WB, Bova GS. Cancer Res. 1998; 58:204–9. [PubMed: 9443392]

Taylor BS, Schultz N, Hieronymus H, Gopalan A, Xiao Y, Carver BS, Arora VK, Kaushik P, Cerami E, Reva B, Antipin Y, Mitsiades N, Landers T, Dolgalev I, Major JE, Wilson M, Socci ND, Lash AE, Heguy A, Eastham JA, Scher HI, Reuter VE, Scardino PT, Sander C, Sawyers CL, Gerald WL. Cancer Cell. 2010; 18:11–22. [PubMed: 20579941]

Villers A, McNeal JE, Freiha FS, Stamey TA. Cancer. 1992; 70:2313–8. [PubMed: 1382830]

Voeller HJ, Sugars LY, Pretlow T, Gelmann EP. J Urol. 1994; 151:492–5. [PubMed: 7904314]

Wang L, Wang WL, Zhang Y, Guo SP, Zhang J, Li QL. Hepatol Res. 2007; 37:389–396. [PubMed: 17441812]

Wang S, Gao J, Lei Q, Rozengurt N, Pritchard C, Jiao J, Thomas GV, Li G, Roy-Burman P, Nelson PS, Liu X, Wu H. Cancer Cell. 2003; 4:209–21. [PubMed: 14522255]

Wang SI, Parsons R, Ittmann M. Clin Cancer Res. 1998; 4:811–5. [PubMed: 9533551]

Wu X, Wu J, Huang J, Powell WC, Zhang J, Matusik RJ, Sangiorgi FO, Maxson RE, Sucov HM, Roy-Burman P. Mech Dev. 2001; 101:61–9. [PubMed: 11231059]

Yeang CH, McCormick F, Levine A. Faseb J. 2008; 22:2605–22. [PubMed: 18434431]

Yoshimoto M, Cunha IW, Coudry RA, Fonseca FP, Torres CH, Soares FA, Squire JA. Br J Cancer. 2007; 97:678–85. [PubMed: 17700571]
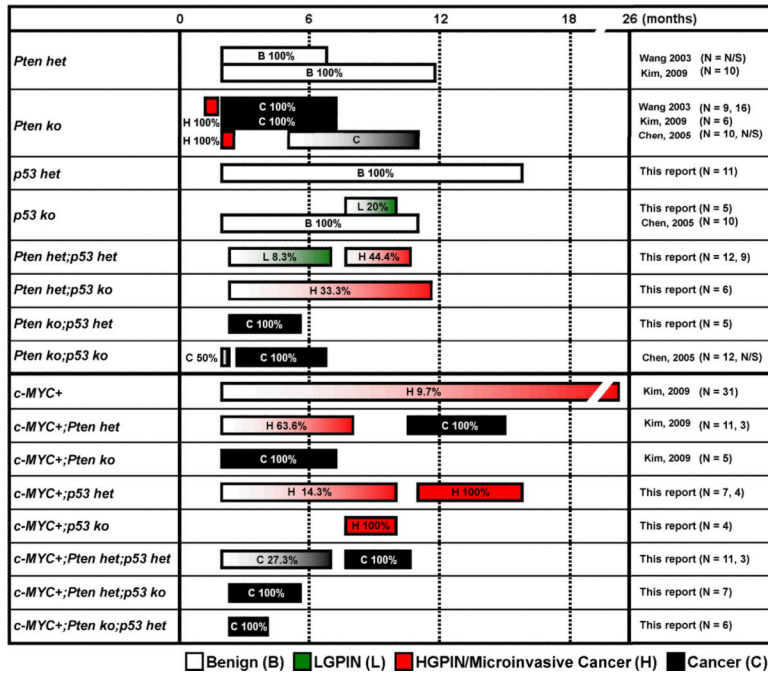
Figure 1. Summarized pathology of mouse prostates with alterations in *c-MYC*, *Pten* and/or *p53*

Pathology summary of prostate-specific, conditional mouse models of prostate cancer with alterations in *c-MYC*, *Pten* and/or *p53*, based on this report and three published studies (Chen et al., 2005; Kim et al., 2009; Wang et al., 2003). The pathological diagnoses are indicated with solid colors when they occur with 100% incidence; otherwise, shown as gradient colors. All the reports utilized the same prostate-specific *Cre* line (*PbCre4*, (Wu et al., 2001)). Het = conditional heterozygous mutant, ko = conditional knockout, N/S = numbers not specified.
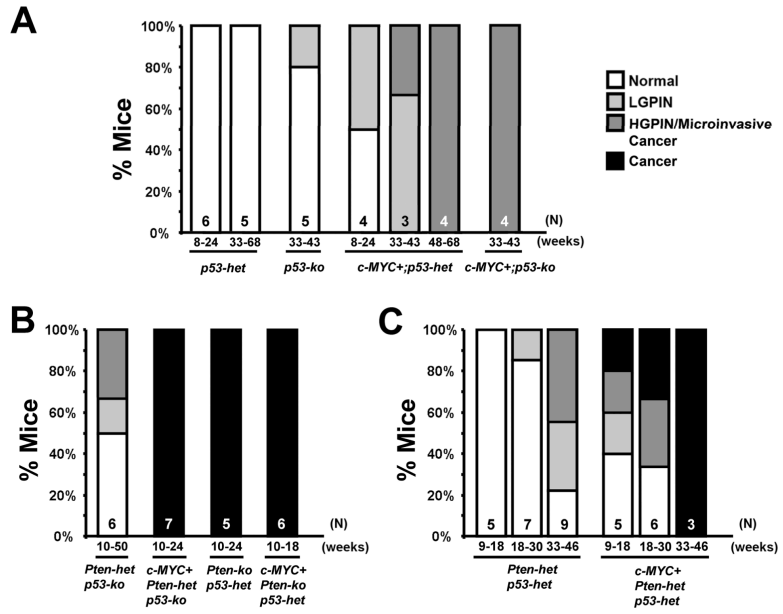
Figure 2. Summary of pathology of mouse prostates
Graphs show histopathology findings in each group of mutant mouse prostates. Genotypes, the number of mice (N) examined and ages (in weeks) when analyzed are indicated.
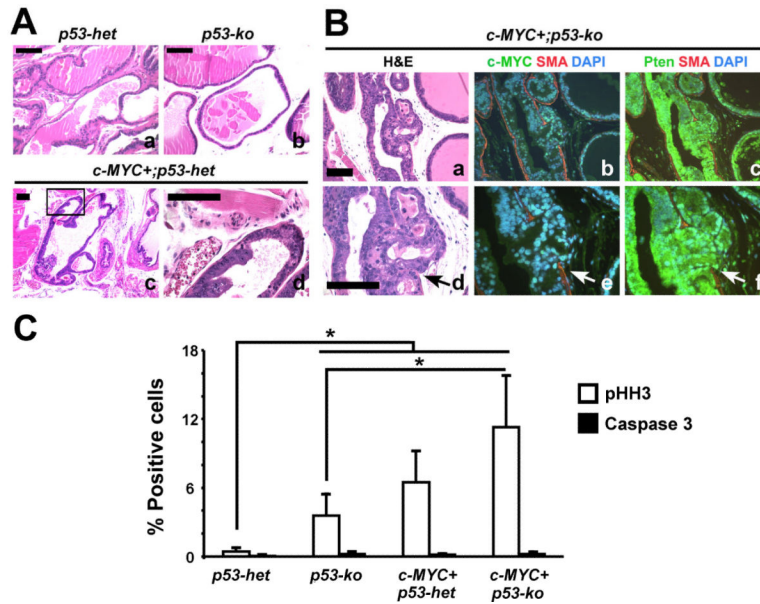
Figure 3. Modest cooperation between focal c-MYC expression and *p53* haploinsufficiency or deficiency in the mouse prostates

(A and B) H&E images showing the pathology in mutant mouse prostates. Note focal high grade PIN in *c-MYC+;p53-het* mouse prostates (`c' and `d' in A) and PIN with microinvasion (arrows) in *c-MYC+;p53-ko* prostate (`a' and `d' in B). Note breach in SMA, smooth muscle actin indicative of microinvasion in `b' and `e'. Panels `c' and `f' in B show Pten expression by immunofluorescence. Scale bars: 100μm. (C) Cellular proliferation and apoptosis in the mouse prostates are quantitated following immunohistochemistry for phospho-histone H3 (pHH3) and activated Caspase 3, respectively. N=3–5 per group. *$P < 0.05$.
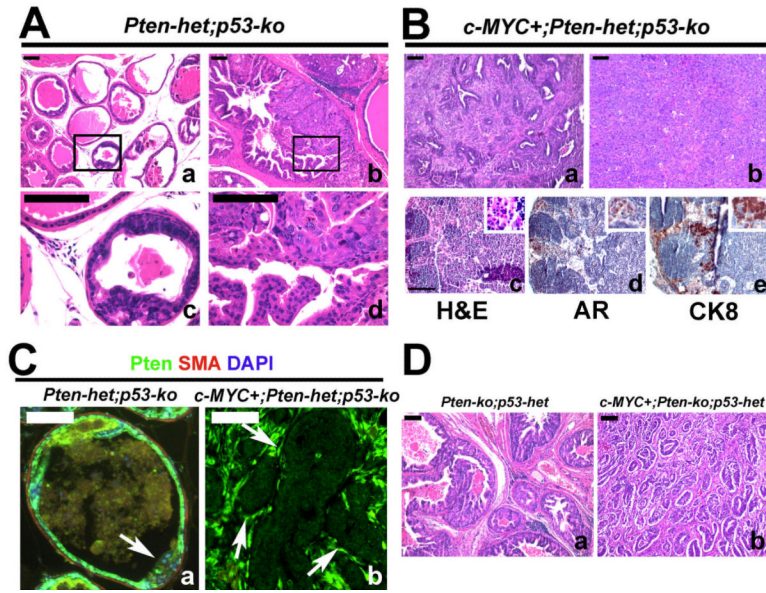
Figure 4. Additional deletion of either one or two copies of *Pten* accelerates tumor formation and leads to lymph node metastases

(A) H&E stains. Examples of rare, focal HGPIN in old *Pten-het;p53-ko* mouse prostate (age=50 weeks) are shown in panels `a–d'. (B) H&E stains of sections from *c-MYC+;Ptenhet;p53-ko* mice show aggressive cancers (panels `a' and `b') with lymph node metastases (panels `c–e'). `c,d,e' show H&E, staining for androgen receptor (AR) and cytokeratin 8 (CK8) in lymph node (insets are higher magnification images). (C) Immunofluorescent detection of focal (a) or diffuse (b) loss of Pten expression (arrows) in mice with the indicated genotypes. (D) H&E stained sections show HGPIN/well-differentiated cancer and moderately-differentiated cancer in *Pten-ko;p53-het* (a) and *c-MYC+;Pten-ko;p53-het* (b) mouse prostates, respectively. Scale bars: 100μm.
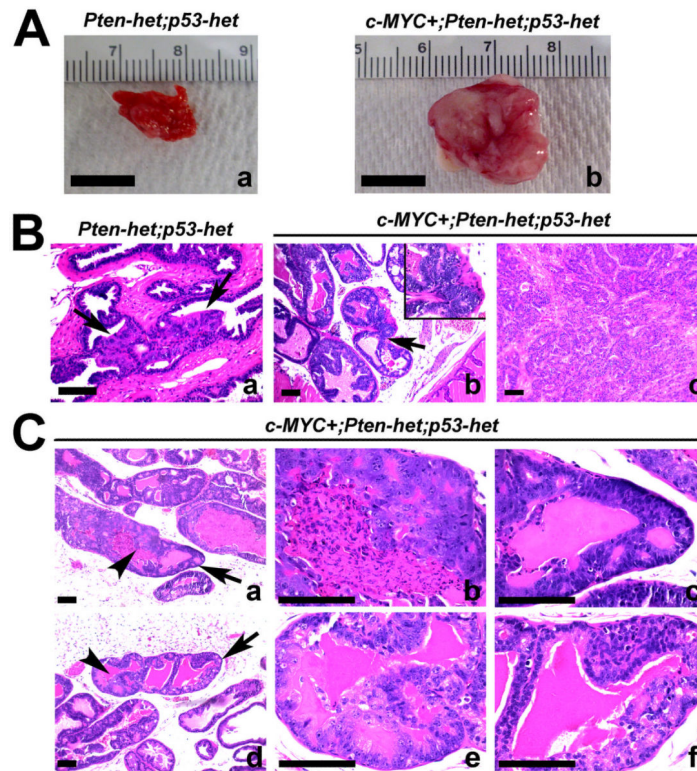
Figure 5. c-MYC+;Pten-het;p53-het mice develop heterogeneous prostate cancer
(A) Gross images of prostates of *Pten-het*;*p53-het* (a) and *c-MYC+*;*Pten-het*;*p53-het* (b) mice. (B) H&E stains show representative pathology of the mouse prostates. Note that only older (33–46 weeks) *Pten-het*;*p53-het* mouse prostates developed mPIN lesions (arrows in `a') while focal invasive (arrow in `b') or poorly differentiated cancer developed in *c-MYC +*;*Pten-het*;*p53-het* mouse prostates. Inset in `b' shows high power image of focal invasion. (C) Heterogeneity in mPIN/cancer lesions of *c-MYC+*;*Pten-het*;*p53-het* mouse prostates. Note lesions marked with arrows and arrowheads showing distinct histology. (`b' and `c' are enlarged portions of the gland shown in `a' while `e' and `f" are enlarged portions of gland shown in `d'). Scale bars: 1cm in "A", 100μm in "B" and "C".
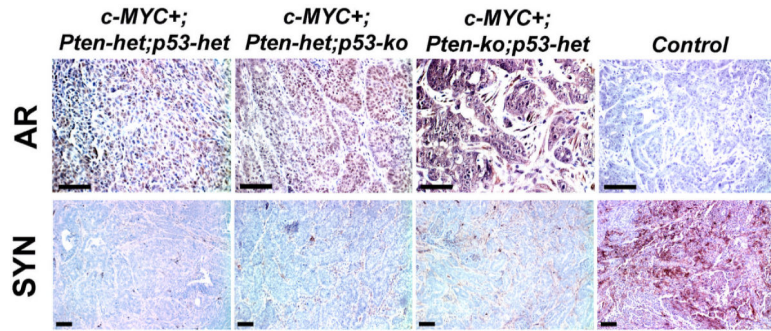
Figure 6. Androgen receptor and synaptophysin expression in mouse prostate tumors
Top, Androgen receptor, (AR) expression is present as brown nuclear and nuclear/
cytoplasmic staining in mutant mouse prostate tumors. Control is a sample without primary
antibody. *Bottom*, Neuroendocrine marker synaptophysin expression (brown) is grossly
absent in mouse prostate tumors. Control is a MYC/Pim1-expressing tumor used as a
positive control. Scale bars, 100μm.
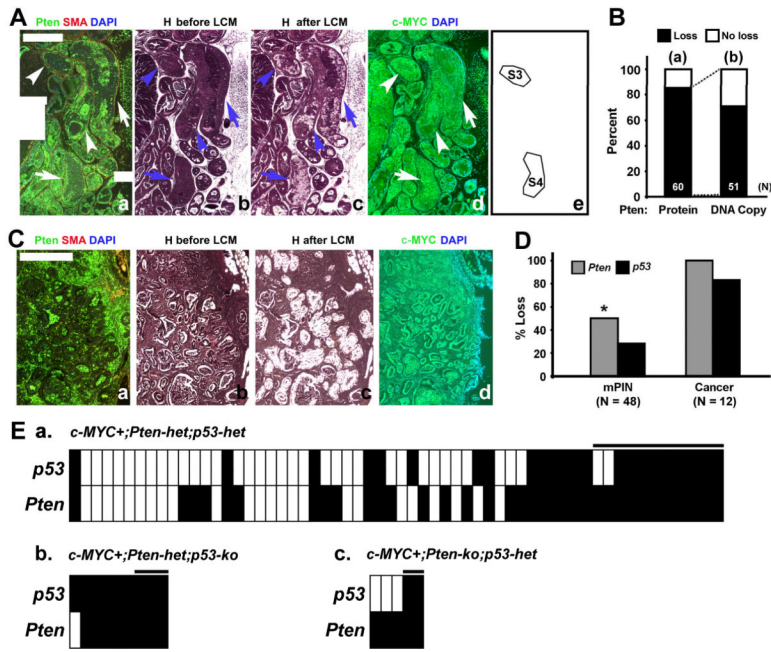
Figure 7. A preference for loss of *Pten* prior to loss of *p53* in c-MYC-initiated mouse prostate cancer

(A and C) Adjacent sections from *c-MYC*+;*Pten-het*;*p53-het* mouse prostates were stained for Pten/SMA, Hematoxylin (H) or c-MYC. PIN and cancer foci were microdissected by LCM and DNA isolated. Arrows indicate microdissected glands. Lesions S3 and S4 (e) both have loss of Pten protein expression but only S4 shows loss of *Pten* DNA copy number. Scale bars: 500μm. (B) Graph showing percent loss of Pten protein expression in abnormal prostatic lesions (N = 60 lesions, including 48 PINs and 12 cancers) analyzed (`a', black bar) and percent of lesions that also lost the wild type *Pten* DNA copy (N = 51) (`b', black bar). (D) Comparison of the frequency of loss of *Pten* or *p53* wild type alleles. Note that *Pten* loss is significantly more frequent than *p53* loss in PIN but not cancer lesions. *Chi*-square test, $P < 0.05$. (E) Heatmap representations of loss of either *Pten* or *p53* loss (black bars) in each sample (PIN and cancer) based on the copy number analysis in Table 1. Boxes under the black line indicate cancer samples, while the remaining samples are PIN. Number of microdissected lesions analyzed: *c-MYC*+;*Pten-het*;*p53-het,* N=60. *c-MYC*+;*Pten-het*;*p53-ko*, N=9 and *c-MYC*+;*Pten-ko*;*p53-het*, N=5.
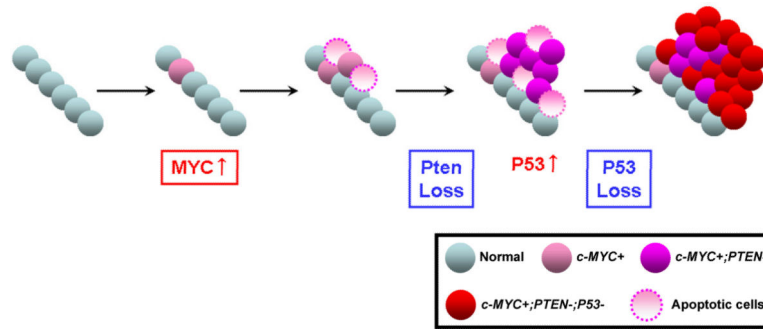
Figure 8. Model for loss ofn *Pten* and *p53* in c-MYC-initiated prostate cancer
c-MYC expression in the prostatic epithelium provokes a mild increase in proliferation and apoptosis. A majority of the c-MYC-expressing cells show no histological abnormality. At this stage, the p53 pathway is not activated. Next, c-MYC-expressing cells preferentially lose the *Pten* tumor suppressor leading to increased proliferation and progression to cancer. However, at this stage apoptosis is also evident due to activation of p53 pathway upon *Pten* loss. Selective pressure to avoid apoptosis promotes loss of *p53*, allowing cells to overcome apoptosis, resulting in development of aggressive prostate cancer.

Table 1

Pten expression status and gene copy number quantitation of *Pten* and *p53* in mutant mouse prostate samples.

Mouse ID (age)	Sample #	Pathology	Pten IHC	Pten Copy #	Normalized Qty (*Ren*)	p53 Copy #	Normalized Qty (*p53*)
c-MYC+;Pten-het;p53-ko							
7352 (16wks)	S55	PIN	-	0	0.1156	0*	ND
	S56	PIN	-	0	0.2928	0*	ND
	S58	Cancer	-	0	0.0446	0*	ND
7345 (17wks)	S52	PIN	-	0	0.1534	0*	ND
	S53	PIN	-	0	0.2352	0*	ND
	S54	Cancer	-	0	0.007	0*	ND
151 (19wks)	S51	PIN	+	1	0.6712	0*	ND
	S49	PIN	-	0	0.1732	0*	ND
	S50	Cancer	-	0	0.1482	0*	ND
c-MYC+;Pten-ko;p53-het							
547 (16wks)	S70	PIN	ND	0*	ND	0	0.2315
	S69	Cancer	ND	0*	ND	0	0.098
593 (18wks)	S100	PIN	ND	0*	ND	1	0.3003
	S101	PIN	ND	0*	ND	1	0.4117
	S102	PIN	ND	0*	ND	1	0.2942
c-MYC+;Pten-het;p53-het							
7312 (10wks)	S19	PIN	-	0	0.0015	0	0.0448
8150 (16wks)	S1	Cancer	-	0	0.3333	1	0.5797
	S2	PIN	-	1	0.6062	1	0.6318
	S3	PIN	-	1	0.6087	1	0.7103

Mouse ID (age)	Sample #	Pathology	Pten IHC	Pten Copy #	Normalized Qty (Ren)	p53 Copy #	Normalized Qty (p53)
	S4	Cancer	-	0	0.3283	1	0.5631
	S5	PIN	+	1	0.9152	1	0.7202
	S6	PIN	+	1	1.0263	1	0.5593
	S7	PIN	+	1	0.9161	1	0.6605
	S8	PIN	+	1	1.0027	1	0.5276
	S10	PIN	+	1	1.3528	1	0.9262
561 (17wks)	S96	PIN	-	1	0.483	1	0.4282
	S97	PIN	-	1	0.5407	1	0.4322
	S98	PIN	-	0	0.3992	1	0.3146
	S99	PIN	-	0	0.4241	1	0.3983
355 (18wks)	S83	PIN	-	0	0.3536	1	0.3051
	S84	PIN	-	1	1.6025	1	0.3974
243 (23wks)	S82	PIN	-	0	0.3355	0	0.236
8184 (24wks)	S11	PIN	-	0	0.2316	1	0.751
	S12	PIN	-	1	0.9762	1	0.6265
	S13	PIN	-	1	0.8407	1	0.6842
	S14	PIN	-	1	0.7727	1	0.7652
	S15	PIN	-	1	0.7679	1	0.701
	S16	PIN	-	1	0.6586	1	0.7117
	S17	PIN	-	1	0.5308	1	0.7464
	S78	PIN	-	0	0.2545	0	0.157
	S79	PIN	-	0	0.2557	1	0.3114
	S80	PIN	-	0	0.2463	1	0.3972
	S81	Cancer	-	0	0.3272	0	0.2112
7367 (26wks)	S28	PIN	+	1	0.4922	1	0.32
	S29	PIN	-	1	0.5657	1	0.483
	S30	PIN	-	0	0.3419	0	0.1239
	S31	PIN	-	0	0.3549	0	0.2659

Mouse ID (age)	Sample #	Pathology	Pten IHC	Pten Copy #	Normalized Qty (Ren)	p53 Copy #	Normalized Qty (p53)
	S32	PIN	-	0	0.2626	1	0.3308
	S34	PIN	-	1	0.552	1	0.3014
	S35	PIN	+	1	0.7529	0	0.2411
	S36	PIN	-	0	0.4428	1	0.3726
	S38	PIN	+	1	0.5998	1	0.3149
	S39	PIN	-	0	0.4191	1	0.2928
	S41	PIN	+	1	0.4396	1	0.4553
	S42	PIN	-	0	0.3313	1	0.6036
	S76	PIN	-	1	0.3464	0	0.2705
	S77	PIN	-	0	0.3299	0	0.2451
411 (27wks)	S93	PIN	-	1	0.4076	1	0.3423
	S94	PIN	-	0	0.4472	1	0.3562
	S95	PIN	-	0	0.4099	1	0.3082
7379 (38wks)	S43	Cancer	-	0	0.0376	0	0.0159
	S44	Cancer	-	0	0.0168	0	0.0078
	S45	Cancer	-	0	0.0815	0	0.018
	S47	PIN	-	0	0.2102	0	0.1327
8409 (39wks)	S22	Cancer	-	0	0.0001	0	0.1290
	S23	Cancer	-	0	0.0009	0	0.0690
	S24	Cancer	-	0	0.0003	0	0.0691
	S25	Cancer	-	0	0.1867	0	0.2615
109 (40wks)	S86	PIN	-	0	0.2649	0	0.2491
	S87	PIN	-	0	0.0777	0	0.0779
	S88	Cancer	-	0	0.0054	0	0.0076
	S89	Cancer	-	0	0.0348	0	0.0223
	S90	PIN	-	0	0.1058	0	0.0563
	S91	PIN	-	0	0.0825	0	0.0771
	S92	PIN	-	0	0.1826	0	0.1242

Gene copy number was determined by qPCR of DNA isolated from immunofluorescence-guided microdissected PIN and cancer lesions.

*
Copy number based on genotype. ND = not determined. Wks = weeks. IHC=immunohistochemistry.